Simulation of Ultrasound Images for Validation of MR to Ultrasound Registration in Neurosurgery

Hassan Rivaz and D. Louis Collins

McConnell Brain Imaging Center
McGill University, Montreal, QC, Canada

Abstract. Image registration is an essential step in creating augmented environments and performing image-guided interventions. Registration algorithms are commonly validated against simulation and real data. Both validations are critical in a comprehensive analysis: On one hand, the simulation data provides ground truth registration results and can therefore accurately measure the performance of algorithms. It is also flexible and can include different levels of noise and outlier data. On the other hand, real data include factors that are not modeled in simulations and is therefore used to test algorithms against real-world applications. Simulated MR images are provided in the BrainWeb database and have been extensively used to validate and improve image registration algorithms. Simulated US images that correspond to these MR images are of great interest due to the growing interest in the use of ultrasound (US) as a real-time modality that can be easily used during interventions. In this work, we first generate digital brain phantoms by distribution of US scatterers based on the tissue probability maps provided in BrainWeb. We then generate US images of these digital phantoms using the publicly available Field II program. We show that these images look similar to the real US images of the brain. Furthermore, since both the US and MR images are simulated from the same tissue probability map, they are perfectly registered. We then deform the digital phantoms to simulate brain deformations that happen during neurosurgery, and generate US images of the deformed phantoms. We provide some examples for the use of such simulated US images for testing and enhancing image registration algorithms.

1 Introduction

An important step in generating augmented reality and image-guided operations is accurate alignment of different images of the tissue, such as magnetic resonance (MR) and ultrasound (US). Since the ground truth alignment between these images is rarely known in real tissue, validation of image registration algorithms is a challenging task. Open access databases that are used for validation include the Retrospective Image Registration Evaluation (RIRE) database [1], which contains MR, CT and positron emission tomography (PET) images of the brain,

and Brain Images of Tumors for Evaluation (BITE) database [2], which provides ultrasound (US) and MR images. To allow validation of registration results, physical fiducials in RIRE or manually selected homologous anatomical landmarks in BITE can be used. While these databases test the algorithms against challenging real images, they have two limitations. First, the fiducial/landmark localization error limits the accuracy of the ground truth. Second, landmarks are limited to few points in the volumes and therefore registration accuracy throughout the volumes cannot be estimated.

Simulated images address these issues, and are usually included as (a necessary, but not sufficient) part of the validation experiments. As an example, the BrainWeb database [3] provides simulated T1-, T2- and proton-density- (PD-) weighted magnetic resonance (MR) images of the brain. The MR images are estimated from a probabilistic brain tissue type probability map. This database has been extensively used for validation of the image registration algorithms, evidenced by over 1200 citations.

Currently, no publicly available simulated dataset is available for testing and validating US registration algorithms. With the rapid growth of US in image-guided interventions and the need to register the intra-operative US (iUS) images to pre-operative acquisitions (commonly MR or CT), simulation of US images is of great importance.

In this work, we simulate realistic US images of brain using the Field II program [4]. Since US is generally used for imaging soft tissue, a deformable registration is needed to accurately register iUS to the pre-operative images in many image-guided surgical/radiotherapy applications. In this paper, we start from tissue probability maps provided in BrainWeb, generate digital US phantoms, and simulate 2D US images of the digital phantom from different orientations. We then deform the digital phantom to simulate brain deformation (i.e. brain shift), and generate US images of the deformed phantom. We generate US images from three simulated craniotomy locations of the brain with three different (zero, small and large) deformation levels. Outlier data is also commonly present in image registration problems; an example is the tumor resection area in the US image that does not correspond to the tumor in the MR image. To simulate the outlier data in US images, we change tissue probability maps at some regions, generating two US images with and without outliers at every location. Finally, at each craniotomy location, we simulate 100 2D US slices separated in the out-of-plane direction by 0.2 mm, similar to BITE database where the 2D handheld probe is swept on the tissue to generate 3D US. We will make this data publicly available.

US simulation is computationally expensive; simulation of a single US slice takes 9 hours on a 3 GHz CPU. Therefore, the total time for simulation of two sequence of 100 US slices corresponding to before and after compression of the phantom takes 75 days. We hope that making this data publicly available speeds testing and improving US registration algorithms.

This paper is organized as follows. In the next section, we elaborate the Field II simulation algorithm, construction of the digital US phantoms with and

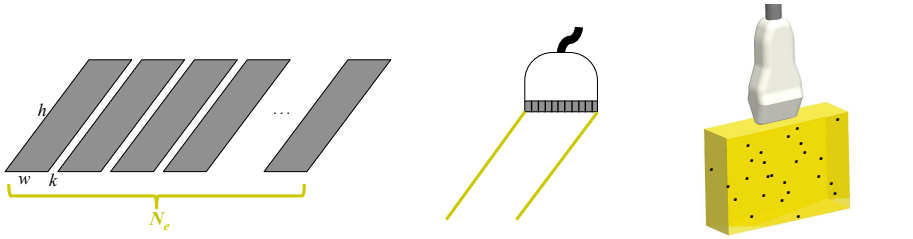

(a) The transducer (b) Steered insonification (c) Point scatterers distributed in 3D

Fig. 1. The transducer and digital phantom. (a) shows the zoomed transducer, consisting of N_e piezoelectric elements with height h, width w and kerf k. (b) shows the a steered insonification. Many such insonifications are performed in different angles to generate the fan-shaped image in phased array probes. (c) shows the digital phantom, where many US scatterers are distributed randomly. We place approximately 8 scatterers per cubic mm in our simulations as suggested by [4].

without outliers and deformation of the US phantoms. We then present the results, followed by conclusions and future work directions.

2 Methods

An ultrasound probe usually consists of many small piezoelectric elements that convert electric voltage to ultrasonic wave (Fig. 1 (a)). Each element is capable of both generating US waves using electric voltage, and listening for wave reflections from the tissue and converting acoustic signals to electrical voltage. To generate a typical 2D B-mode US image, a most basic strategy would be to generate one line from each element. However, some (or all) of the elements are excited together with pre-calculated time delay and amplitude to focus the beam at a desired location or to steer it in a desired direction (Fig. 1 (b)). Similarly, when the acoustic reflection is received in multiple elements, pre-specified delays and gains are used to average the signals. Transmit and receive focusing and steering are referred to as *beamforming* and significantly improve the quality of US images. We set all N_e elements in Field II simulations as active elements for beamforming to generate high quality images.

Each piezoelectric element at the US probe generates acoustic pressure in the form of a short sinusoidal pulse modulated with a Hanning or Gaussian window function. We use a Gaussian modulated excitation:

$$e(t) = \exp\left(-\frac{(t-\mu)^2}{2\sigma^2}\right) \cdot \sin(2\pi f_0 t) \tag{1}$$

where t is time, f_0 is the probe's center frequency, μ is the mean and σ^2 is the variance of the Gaussian function. Let $g(-\mathbf{x}, t)$ be the impulse response of the

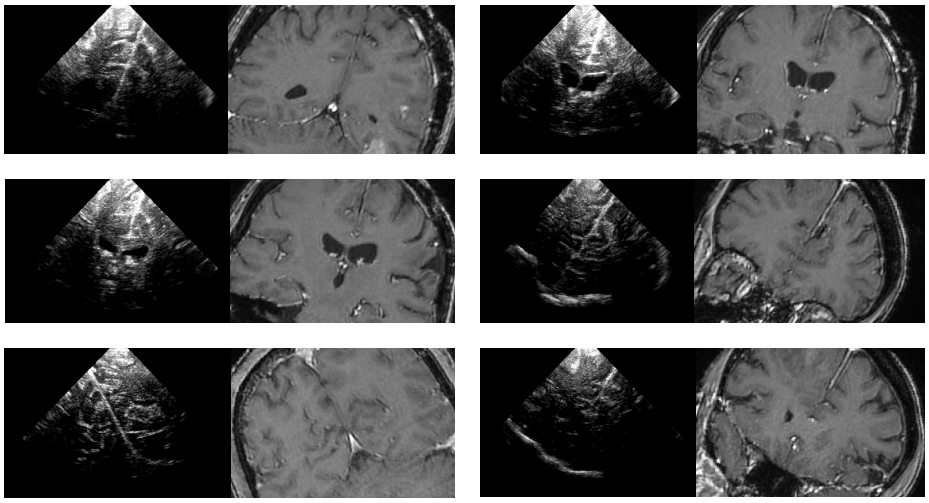

Fig. 2. Six examples of the intra-operative B-mode US and the corresponding pre-operative MR images from the BITE database. Note that the sulci and ventricles appear respectively hyperechoic and hypoechoic in the US images.

transducer, i.e. the pressure field generated from a Dirac delta excitation at the transducer at location $\mathbf{x}$ and time t. Field II performs the following convolution to calculate the radio-frequency (RF) data $r(\mathbf{x_0}, t)$ at a particular point $\mathbf{x_0}$ and time t [5,6]:

$$r(\mathbf{x_0}, t) = e(t) \underset{t}{*} g(-\mathbf{x}, t) \underset{\mathbf{x}}{*} s(\mathbf{x}) \Big|_{\mathbf{x}=\mathbf{x_0}} \tag{2}$$

where $\underset{t}{*}$ and $\underset{\mathbf{x}}{*}$ respectively denote temporal and spatial convolution, and s is the scattering medium. Field II allows placement of point scatterers with the desired scattering amplitude and location in the medium (e.g. Fig. 1 (c)). In the next section, we describe how we distribute scatterers in the brain phantom.

2.1 Scatterer Distribution

A portion of the US wave gets reflected when the acoustic impedance of the medium changes. Part of this reflection is because of microscopic changes in tissue properties, which is referred to as diffuse scattering. Another part is due to changes at the macroscopic level, e.g. at the boundary of gray matter (GM) and cerebrospinal fluid (CSF) (see [7] for more details). We incorporate both reflection sources in our digital brain phantom.

To model diffuse scattering, we spread many point scatterers (8 per cubic mm) throughout the phantom with normally distributed scattering amplitude. The scattering properties of white matter (WM), GM and CSF are different. Therefore, we follow previous work [8] that simulates US images from MRI.

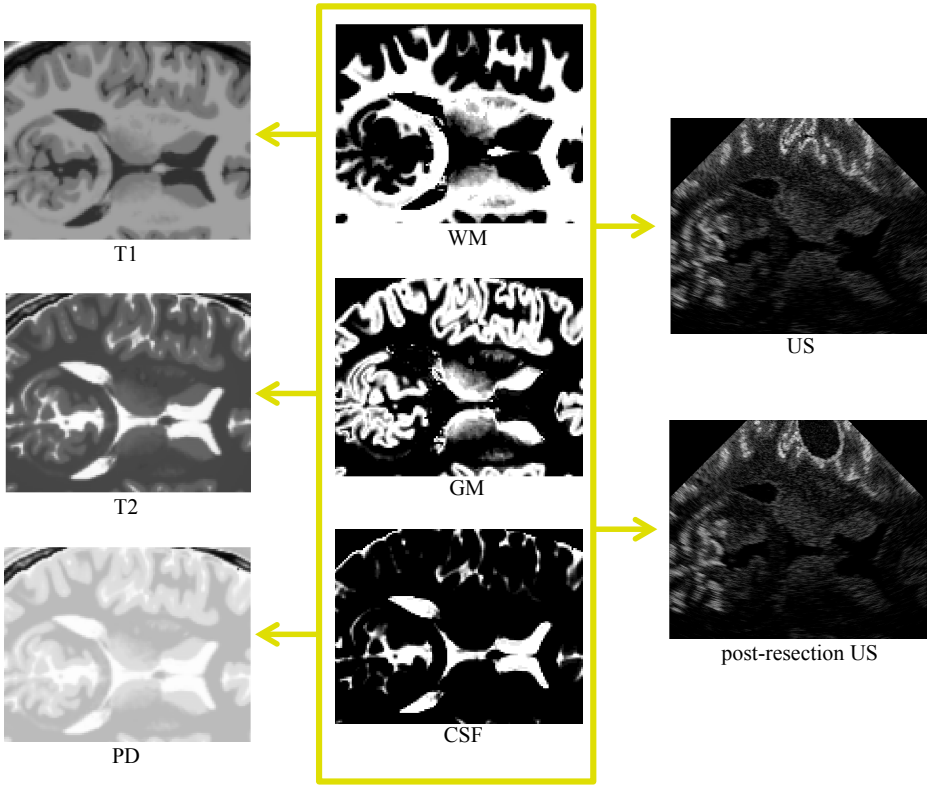

Fig. 3. Simulation of MR and US images from tissue probability maps in the middle column. Parts of the WM, GM and CSF are altered in the post-resection US image to simulate tissue resection.

They suggest the intensity values of 32, 12 and 4 for respectively GM, WM and CSF, and show that the simulated US images can be registered to real US images using cross correlation. Hence, we multiply the amplitude of scatterers intensity by these values based on their probabilistic tissue type determined by the BrainWeb phantom.

The ratio of US wave reflected at the boundary between two tissues with acoustic impedances Z_1 and Z_2 is $(Z_1 - Z_2)^2/(Z_1 + Z_2)^2 \cdot \cos(\theta)$, where θ is the incident angle. We calculate θ at every boundary by performing a dot product between the radial US wave and the normal of CSF tissue probability map edges[1]. Since acoustic impedance values for different brain tissue types are not available, we use the BITE database to approximate the reflection values. We

[1] Since the boundary between WM and GM is not generally sharp, it is usually not visible under US. However, the boundary between CSF and WM or GM is sharp and is visible in US, and therefore we only consider CSF edges.

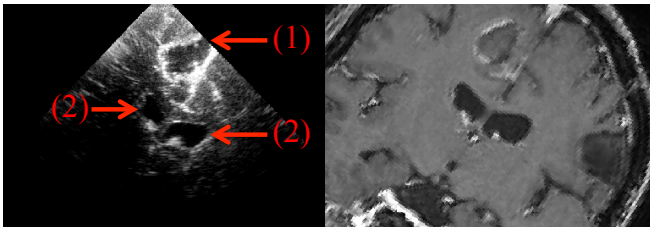

Fig. 4. Post-resection US and pre-operative MR images of neurosurgery. (1) and (2) respectively refer to the resection cavity and ventricles. The tumor region in MR does not correspond to the resection cavity in US.

therefore multiply scatterer intensities by the gradient magnitude of CSF tissue probability. The reflection at sulci CSF is significantly stronger compared to the CSF boundary at the ventricle regions (see Fig. 2). Previous work [9] has in fact used this enhancement to perform US-MR registration. We therefore locate sulci area using morphological operations, followed by manual correction, and further multiply the amplitude of scatterers at CSF boundaries at sulci by 32. We select this number by investigating images from the BITE database. It should be noted that based on time gain control (TGC) and other factors, the US intensity at sulci can be different. Therefore, there is no perfect number for intensity values selected in this work. Fig. 3 shows the tissue probability maps and T1, T2 and PD weighted MR images from the BrainWeb, along with the simulated US image. Since both US and MR images are simulated from the same tissue probability map, they are aligned. In the next section, we alter the tissue probability maps to generate US images with outliers.

2.2 US Images With Outliers

Tumor resection and bleeding are among the sources of outliers when registering US and MR images of the BITE database. We simulate tumor resection by changing the WM, GM and CSF tissue types inside an elliptical region to a new hypoechoic type that contains weak scatterers. This is in accordance with real data where the resection region is filled with saline solution and diluted blood (i.e. a weak scattering mixture). We set the scatterer intensity in the resected region to 6 to simulate images that look similar to real images. Another source of artifact in the post-resection US images comes from Surgicel (Ethicon, Somerville, NJ), a surgical hemostat that is often used after resection to stop bleeding. Surgicel generates bright edges around the tumor as shown in Fig. 4. We model this edges in our simulations by placing scatterers around the resection cavity.

2.3 Deformation of the Simulated Phantoms

The brain tissue deforms after the craniotomy and during the surgery due to biochemical and physical factors. The deformation can be as much as 38 mm [10] in some areas. We deform the digital US phantom, by moving its scatterers, using free-form B-spline transformations. In real brain deformation, the maximum displacement of the brain happen around the cortex where craniotomy is performed. We therefore linearly decrease the deformation of the B-spline nodes from the cortex to achieve the deformation shown in Fig. 5 (b). Other deformations that use finite element simulation of viscoelastic tissue models are also possible. It should be noted that we deform the digital phantom (i.e. displace scatterers) and not the BrainWeb tissue probability maps. This is in accordance with reality, where the scatterers move with the brain as it deforms. We deform the digital phantom at two levels with maximum deformation levels of 5 mm and 40 mm.

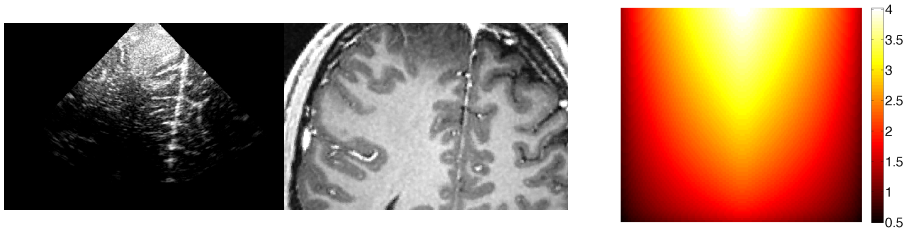

(a) US and MR images (b) Deformation in cm

Fig. 5. The US and MR images in (a) are from the BITE database. The simulated deformation in (b) is the highest close to the cortex (top center), where brain shift is usually the largest.

Table 1. Imaging and US probe parameters (see also Fig. 1).

symbol	description	value
w	width of elements	0.11 mm
h	height of elements	5 mm
k	kerf (dist. between elements)	0.011 mm
N_e	number of all elements	128
N_a	number of active elements	128
f_0	center frequency	7 MHz
f_s	sampling frequency	100 MHz
α	attenuation	35 dB/m
α_{f0}	attenuation center frequency	7 MHz
α_f	frequency dependent attenuation	5 dB/(MHz.m)

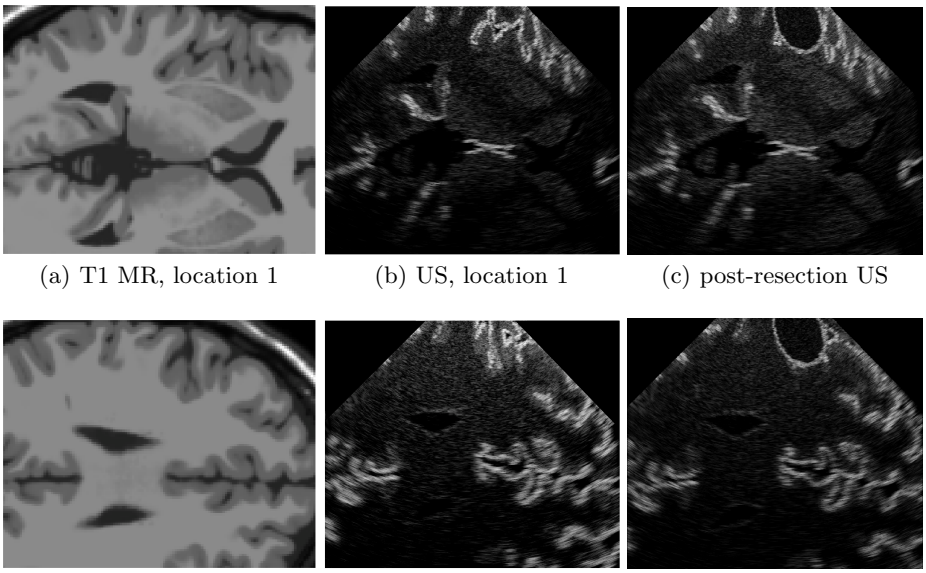

(a) T1 MR, location 1 (b) US, location 1 (c) post-resection US

(d) T1 MR, location 2 (e) US, location 2 (f) post-resection US

Fig. 6. The simulated US images at two different locations. The T1 images are from the BrainWeb. The post-resection US images simulate tumor resection and contain outlier data.

2.4 Simulation Time

Simulation of a single US slice takes 9 hours on a 3 GHz CPU. Therefore, simulating 100 slices of a sweep takes 37 days. We simulate US slices in 3 locations with 3 different levels of compression (zero, small and large) with 2 different phantoms with and without the resection cavity. Therefore, the total computation time is $3 \times 3 \times 2 \times 37 = 675$ days. Providing this data online can help the academic and industrial research groups in testing and validating novel image registration algorithms.

3 Results

The size of the piezoelectric elements and their distance (Fig. 1) are confidential manufacturer information. We therefore use the values provided in Field II: $w = 0.11$ mm, $h = 5$ mm, $k = 0.011$ mm and $N_e = 128$ (see Fig. 1). We also set the probe's center frequency f_0 to 7 MHz, the sampling frequency f_s to 100 MHz, the focal point of transmitted wave to half of the image depth, and use all $N_e = 128$ elements for transmit and receive beamforming. The value of these parameters are summarized in Table 1.

Field II generates RF data, which is not suitable for visualization because it is modulated with a high frequency ($f_0 = 7$ MHz) carrier (see [11] for more details). Therefore, we calculate the envelope of the RF signal and perform a log compression of the resulting amplitudes to reduce the dynamic range of the envelope. The resulting image is similar to what is commonly seen as a B-mode image on a US scanner. We have simulated US images from three different locations of the brain. Fig. 6 shows the simulated US images, along with BrainWeb T1 MR images, at two locations (the third location is shown in Fig. 3).

The digital phantom is in 3D, and we simulate series of 2D US images that sweep the 3D phantom, similar to the BITE database. The sweeps of 2D US images can then be simply stacked together to generate 3D US volumes.

4 Discussion

Simulated US images can be used to test and validate numerous kinds of image analysis algorithms. First, the deformed US volume and the T1 (or T2 or PD) MR volume can be used to test 3D volumetric registration algorithms. Second, the individual US images and the T1 (or T2 or PD) MR volume can be used to test 2D-3D (i.e. slice to volume) registration algorithms. Third, the post-resection US images and the MR volume can be used to test the robustness of registration algorithms to outlier data. Forth, the US images with and without deformation can be used to test US-US registration algorithms. Fifth, the US images with the small deformation magnitude, the US images with the large deformation magnitude and the MR images can be used to test group-wise registration algorithms, where all three volumes are considered simultaneously to improve the accuracy and robustness of registration algorithm.

The deformation model using the free-form B-splines is purely geometrical and does not respect the mechanical properties of the brain. For example, the deformation of the fluid CSF is fundamentally different from that of WM and GM. Finite element analysis has been used in the past to generate deformation fields that take into account tissue mechanical properties [12,13]. Similar analysis can be used to generate more realistic brain shift deformation maps.

The intensity of B-mode image in different regions of the brain are provided in [8], which we used to set the scatterer amplitudes. However, the relationship between the scatterer intensity and B-mode intensity is rather complex and subject of research [14,15,6]. Nevertheless, these values produced simulated images that are visually similar to the real images from the BITE database. Rigorous validation of the simulated images is a subject of future work.

5 Conclusions

Validation is a critical and challenging step in the development of novel image registration algorithms. In this work, we showed how realistic US images can be simulated from tissue probability maps of the BrainWeb database. Along with the BrainWeb database that provides MR images with different noise and

intensity non-uniformity levels, the simulated US images can be used to test and improve various types of image registration algorithms.

References

1. West, J., Fitzpatrick, J.M., Wang, M.Y., Dawant, B.M., Maurer Jr, C.R., Kessler, R.M., Maciunas, R.J., Barillot, C., Lemoine, D., Collignon, A., et al.: Comparison and evaluation of retrospective intermodality brain image registration techniques. Journal of Computer Assisted Tomography **21** (1997) 554–568
2. Mercier, L., Del Maestro, R.F., Petrecca, K., Araujo, D., Haegelen, C., Collins, D.L.: Online database of clinical MR and ultrasound images of brain tumors. Medical Physics **39** (2012) 3253
3. Collins, D.L., Zijdenbos, A., Kollokian, V., Sled, J., Kabani, N., Holmes, C., Evans, A.: Design and construction of a realistic digital brain phantom. IEEE Trans. Medical Imag **17** (1998) 463–468
4. Jensen, J.A.: Field: A program for simulating ultrasound systems. In: 10th Nordicbaltic conference on biomedical imaging, vol. 4, supplement 1, part 1: 351–353, Citeseer (1996)
5. Jensen, J.A.: A model for the propagation and scattering of ultrasound in tissue. The Journal of the Acoustical Society of America **89** (1991) 182
6. Afsham, N., Najafi, M., Abolmaesumi, P., Rohling, R.: A generalized correlation-based model for out-of-plane motion estimation in freehand ultrasound. (2013)
7. Hedrick, W.R., Hykes, D.L., Starchman, D.E.: Ultrasound physics and instrumentation. Mosby St. Louis (1995)
8. Mercier, L., Fonov, V., Haegelen, C., Del Maestro, R.F., Petrecca, K., Collins, D.L.: Comparing two approaches to rigid registration of three-dimensional ultrasound and magnetic resonance images for neurosurgery. International journal of computer assisted radiology and surgery **7** (2012) 125–136
9. Coupé, P., Hellier, P., Morandi, X., Barillot, C.: 3D rigid registration of intraoperative ultrasound and preoperative mr brain images based on hyperechogenic structures. Journal of Biomedical Imaging **2012** (2012) 1
10. Nabavi, A., Black, P., et al.: Serial intraoperative magnetic resonance imaging of brain shift. Neurosurgery **48** (2001) 787–798
11. Wachinger, C., Klein, T., Navab, N.: The 2D analytic signal for envelope detection and feature extraction on ultrasound images. Medical Image Analysis **16** (2012) 1073–1084
12. Dumpuri, P., Thompson, R.C., Dawant, B.M., Cao, A., Miga, M.I.: An atlas-based method to compensate for brain shift: Preliminary results. Medical Image Analysis **11** (2007) 128–145
13. Rivaz, H., Boctor, E.M., Choti, M.A., Hager, G.D.: Real-time regularized ultrasound elastography. Medical Imaging, IEEE Transactions on **30** (2011) 928–945
14. Mohana Shankar, P., Dumane, V., Reid, J.M., Genis, V., Forsberg, F., Piccoli, C.W., Goldberg, B.B.: Classification of ultrasonic b-mode images of breast masses using nakagami distribution. Ultrasonics, Ferroelectrics and Frequency Control, IEEE Transactions on **48** (2001) 569–580
15. Seabra, J., Sanches, J.: Modeling log-compressed ultrasound images for radio frequency signal recovery. In: 30th Annual International Conference of the IEEE, Engineering in Medicine and Biology Society (EMBS 2008). (2008)